ACS APPLIED MATERIALS & INTERFACES

Research Article

www.acsami.org

Electrorheology of Suspensions Containing Interfacially Active Constituents

Carl McIntyre,[†,∥] Hengxi Yang,[‡] and Peter F. Green*[,†,§]

[†]Department of Material Science and Engineering, [‡]Department of Physics, and [§]Department of Chemical Engineering, University of Michigan, Ann Arbor, Michigan 48109, United States

Supporting Information

ABSTRACT: We recently showed that a suspension of micrometer-sized polystyrene (PS) particles in a PDMS liquid, mixed with small (1 wt %) amounts of a nanocage, sulfonated polyhedral oligomeric silsesquioxane (s-POSS), exhibited significant electrorheological (ER) behavior. This behavior was associated with the formation of a thin adsorbed layer of s-POSS onto the surfaces of PS and the subsequent formation of polarization-induced aggregates, or structures, responsible for the ER effect in an applied electric, *E*, field. Current theory suggests that the ER effect would largely be determined by the dielectric and conductive properties of the conductive layer of core/shell particles in ER suspensions. We show here that sulfonated-PS (s-PS)/PDMS suspensions exhibit further increases in the yield stress of over 200%, with the addition of s-POSS. The yield stress of this system, moreover, scales as $\tau_y \propto E^2$. The dielectric relaxation studies reveal the existence of a new relaxation peak in the s-POSS/s-PS/PDMS system that is absent in the s-POSS/PS/PDMS suspension. The relative sizes of these peaks are sensitive to the concentration of s-POSS and are associated with changes in the ER behavior. The properties of this class of ER fluids are not appropriately rationalized in terms of current theories.

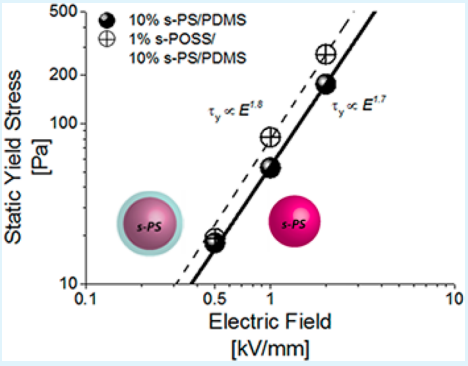

KEYWORDS: *electrorheological fluid, colloids, core/shell particles, stimuli-responsive materials, self-assembly*

INTRODUCTION

The archetypal electrorheological (ER) suspension is composed of a single phase of polarizable particles within an insulating liquid phase, typically an oil. The ER effect occurs when the suspension is placed in an electric field, *E*, and the *E*-field induced polarizable particles self-assemble to form a mesostructure, highly oriented in the direction of the field.[1,2] The material exhibits reversible changes of the apparent viscosity by up to 3 orders of magnitude in the presence of the field. Several attempts have been made to design ER fluids with higher viscosities under an electric field, by considering materials of different chemical structures. Researchers, for example, have shown that the addition of acids and surfactants may enhance the ER effect, manifested through increases in the yield stress or enhancements of the stability of the suspension under sufficiently high electric fields.[3−6] These additives have the effect of increasing the strength of particle interactions within the *E*-field induced oriented mesostructures. Such compounds either form surface bridges to increase the cohesion of the active mesostructures or they change conductive properties (i.e., increasing the polarization) of these mesostructures. The viability of these strategies has important implications for the design of smart fluids composed of nano- and macro-scale particles.

Other effective strategies for increasing the ER response of a suspension include coating the surfaces of particles using a more conductive material.[7−10] This enhances the conductivity and permittivity of the particles in relation to the medium, which thereby increases the ER response.[11] The coated layer should be thin, but not sufficiently thin that electric breakdown would occur in the film during the application of the electric field.[8] In a recent publication, we showed that otherwise ER inactive suspensions of micrometer-sized polystyrene (PS) particles in polydimethyl siloxane (PDMS), when mixed with small concentrations of s-POSS, (∼1 wt %) exhibited significant ER activity. We showed that the enhancement is associated with the preferential (interfacial) adsorption of s-POSS onto the surfaces of the s-PS particles in the suspension. This led to the polarization-induced formation of particle aggregates in the presence of the applied field, which was responsible for the yield stress exhibited by the fluid. We report here a significant enhancement, over 90 Pa (∼200%) at moderate fields, of the ER response of a sulfonated polystyrene (s-PS)/PDMS ER suspension due to the addition of sulfonated POSS of weight fractions between 0.5 and 3.0 wt %. This observation is in contrast to current predictions which show that the shell, or coating, of the particles in the suspension is largely responsible for the ER behavior of the suspension.[7−10,12] The dielectric relaxation spectrum of the s-POSS/s-PS/PDMS shows the appearance of a new relaxation peak, which is not present in the

Received: May 10, 2013
Accepted: August 26, 2013
Published: August 26, 2013

   dx.doi.org/10.1021/am4017544 | ACS Appl. Mater. Interfaces 2013, 5, 8925−8931

s-POSS/PS/PDMS system. The magnitudes of both peaks are sensitive to the concentration of s-POSS. The ER effect is largest for concentrations of ~1−2wt % s-POSS. For the larger concentrations of s-POSS, ~3 wt %, the ER effect diminishes. At compositions beyond 2 wt % the magnitude of the new relaxation peak remains constant, whereas the first, primary, relaxation peak, diminishes appreciably with increasing s-POSS. These results indicate that for this class of ER-fluids, with the shell layer formation due to adsorption, is sensitive to the properties of the core (s-PS) and to the adsorbed shell layer. The behavior of this system cannot be appropriately rationalized in terms of current ER theories.

EXPERIMENTAL SECTION

Materials. *ER Fluid Preparation.* Tris Sulfonic Acid Isobutyl POSS (Figure 1) was purchased from Hybrid Plastics and the sodium polystyrene sulfonate powder and PDMS were both purchased from Sigma Aldrich.

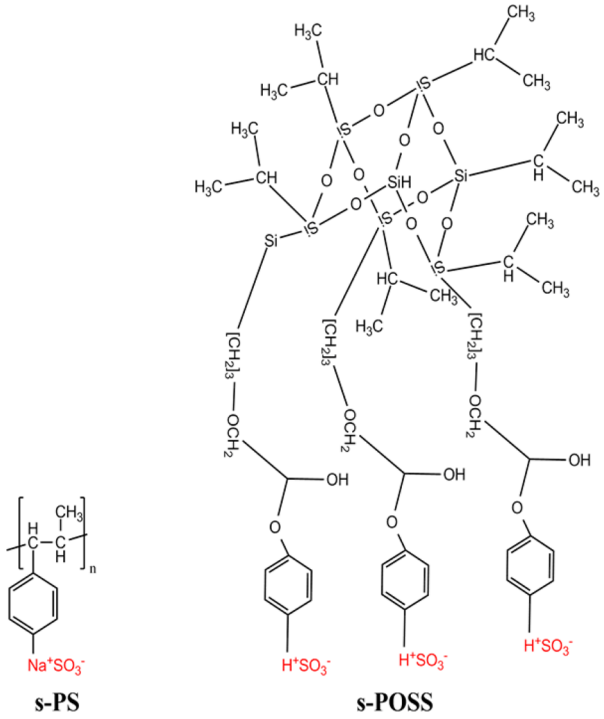

Figure 1. Chemical Structures of Sulfonated Polystyrene (s-PS) and Sulfonated Polyhedral Oligomeric Silsesquioxane (s-POSS).

Drying. Previous research has shown that the presence of absorbed water on the particulate phase of many common "wet" ER fluids is essential to the performance of the ER fluid, and "dry" ER fluids exist that have been shown to function without the presence of water in detectable amounts. Two types of water that can exist in the particulate phase are surface water and structured water. The surface water can be eliminated through routine drying of the particulate phase while structured water requires extensive measures to eliminate.

It is standard procedure for preparing ER fluid to perform routine drying of both the oil or the continuous phase, and the particulates or the dispersed phase. For this study the following measures were carefully followed to minimize the surface water present within the ER fluids. First both the s-PS and POSS heated at 80 °C (sPOSS did not withstand higher temperatures for long periods) under vacuum within a vacuum oven. The PDMS oil was also dried at 150 °C, then transferred into a sealed container in the presence of molecular sieves. The vials containing the dried s-PS and sPOSS were quickly capped upon removal from the vacuum oven. The PDMS was then promptly added to avoid exposure to moisture in the air. The vial mixtures were then capped and stirred. All ER formulations contained 10% wt. s-PS powder in PDMS. The s-POSS concentrations in suspensions varied from 0.5% wt. to 3.0% wt. The average Heywood diameter of the dry powders obtained by microscopy was 19.2 μm. The particle size distribution is available in the Supporting Information. sPOSS/sPS/PDMS mixtures should be stable in electric fields since both sPS/PDMS, which is an industrial ER fluid, and sPOSS/PDMS mixtures were determined to be stable in electric fields from our previous published work.[10]

Methods. *Dielectric Spectroscopy.* The dielectric properties of the suspensions were measured using a broadband dielectric spectrometer (Novocontrol Technologies, GmbH), equipped with a liquid measurement cell containing a gap measuring 6.5 mm and consisting of two metal electrodes (diameter = 12.7 mm) separated by a Teflon spacer. The baseline was determined from data obtained through measurements of the cell filled with PDMS oil. The measurements were performed at a temperature of 25 °C and at frequencies from 0.1 Hz to 10 MHz.

Electrorheology Measurement. The stress−strain rate measurements for the ER suspensions were collected using a strain-controlled rheometer (TA Instruments ARES). Measurements were performed using 50 mm diameter parallel plate geometries. The shear rates in steady rate sweep tests ranged from 0.1 to 30 s^{-1}. To create high electric fields within the ER suspension the rheometer was attached to a DC high voltage generator (Trek Model 609) connected to a 5 MHz function generator (BK Precision 4011A) allowing for voltages up to 4 kV. To ensure homogeneity all samples were initially sheared at high shear rates. To ensure consistency and to prevent stiction,[18] our initial shear rate sweeps were performed at high frequencies; they were subsequently performed at progressively lower frequencies. Yield stresses were obtained, as is the common practice in the field, by fitting the shear stress vs strain rate data to 2 data models using OriginLab. Images of the ER fluid were taken, using an optical microscope, while the fluid was located on a transparent substrate between electrodes surface. The electrodes were connected to a portable high voltage supply with very low current.

RESULTS AND DISCUSSION

An ER fluid is capable of sustaining shear stresses without flowing in the presence of an applied electric field.[14] Optical images of our ER fluid in the presence of an applied electric field are shown in Figure 2. The field-induced structures, or aggregates, span the electrodes; the arrow at the top of the figure identifies the direction of the field. The fluid behaves as a plastic material; it exhibits little or no deformation if the magnitude of the shear stress is less than the yield stress, τ_y. When the applied stress is greater than the yield stress the electrostatic dipole forces responsible for holding the mesostructures spanning the plates together are overcome. Subsequently the particle aggregates rupture, and the ER fluid flows.

The dependence of the yield stresses of the s-PS/PDMS and the s-POSS/s-PS/PDMS suspensions on the applied electric fields, E, is shown in Figure 3. It is evident that the static yield stress of the s-POSS/s-PS/PDMS system increases with the electric field, E: τ_y vs $E^{1.8}$. The magnitude of response of the s-PS/PDMS suspension is not only weaker, but it also exhibits a weaker dependence on the E-field, τ_y vs $E^{1.7}$.

Electrorheological Analysis. The yield stress denotes the sharp transition at which the viscosity of the substance undergoes a transition from "infinitely" high, or solid-like, to liquid-like. This solid-like to liquid-like transition is the basis of the Bingham model. The ideal Bingham Body, in the solid state, possesses an infinite viscosity at stresses below the Bingham yield stress, $\tau_{Bingham}$; above the Bingham yield stress the fluid

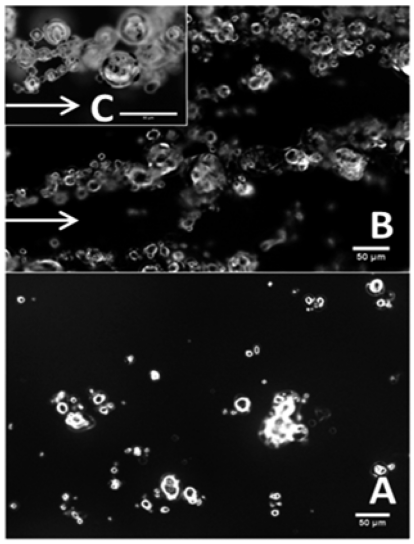

Figure 2. Optical Micrographs (8×) showing s-PS particles in PDMS for 10% s-PS/PDMS ER fluid in the absence of (part A) and under the influence of (part B) an applied electric field. The scale bar is 50 μm. Part C is a magnified, 32×, view of the image in part B. The white arrows indicate the direction of the electric field (E = 800 V/mm).

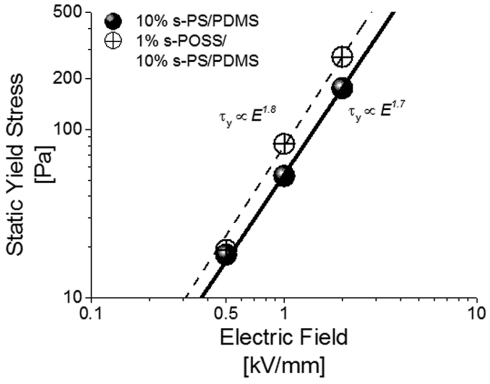

Figure 3. Static yield stress is plotted as a function of the applied electric field, for s-PS/PDMS and for s-POSS (1 wt %)/s-PS/PDMS ER suspensions.

flows with a plastic viscosity,η_∞. The Bingham equation indicates that the shear stress τ is[1]

$$\tau = \left[\frac{\tau_{\text{Bingham}}}{\dot{\gamma}} + \eta_\infty\right]\dot{\gamma} \quad (1)$$

While the Bingham Model appropriately describes the yield stress of an ideal ER fluid, a more complete understanding of yielding in ER fluids often requires a more realistic description of the transition between the solid-like to liquid regimes. The complicated shear behavior of ER fluids subjected to electric fields can include effects such as "trembling" of the shear stress (increase and decrease of the shear stress with shear rate) and thixotropy or time-dependent changes of the viscosity. Empirical models such at the Seo-Seo model describe yielding of ER fluids; they provide a more realistic account of effects such as "trembling".[15] The Seo-Seo model predicts that

$$\tau = \left[\frac{\tau_{sy}}{\dot{\gamma}}\left(1 - \frac{(1 - e^{-A\dot{\gamma}})}{1 + A\dot{\gamma}^{\alpha}}\right) + \eta_\infty\right]\dot{\gamma} \quad (2)$$

In this equation the static yield stress, which measures the stress at which the smart fluid in the electric field begins to flow, is denoted τ_{sy}. The critical strain rate above which the fluid flows with plastic viscosity, η_∞, is $\gamma_c^{-1} = [A]^{-1}$ (lowercase a is also used); α is an empirical parameter. The critical shear rate measured as A^{-1} denotes the point that the stress is no longer linear with the shear rate. We calculated the static yield stress using the Seo-Seo Model. The Bingham yield stress, a measure of the stress at which the smart fluid ceases flowing, was calculated using the Bingham model.

The shear stresses are plotted as a function of shear rates in Figure 4 for the 10 wt % s-PS/PDMS samples. The solid lines

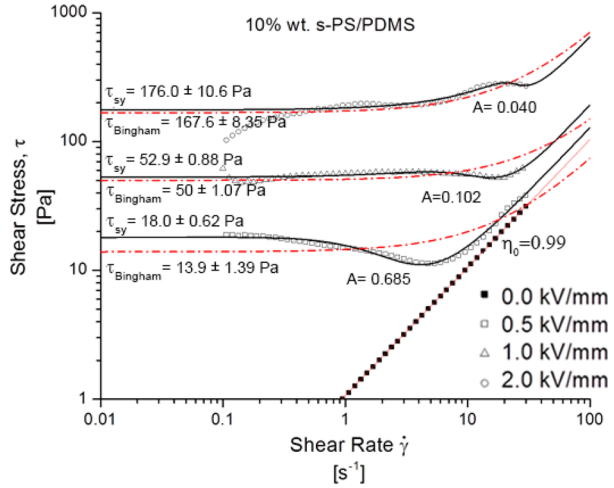

Figure 4. Shear Stress vs Strain Rate for Sulfonated Polystyrene/Polydimethylsiloxane; subjected to different electric fields. The solid straight curves are fits to the Seo-Seo model. The dashed curves are fits to the Bingham Model. The dotted line has a slope of unity. Confidence Intervals (95%) are included for the yield stress values based on the fitting.

were computed using the Seo-Seo model, and the broken lines were calculated using the Bingham model, using the data throughout the entire range. The Bingham yield stress decreases at low shear rates, while the static yield stress remains unaffected (Figure 5).

The values of yield stress of the s-PS/PDMS ER fluid, however, differ by less than 6.0% between those predicted by both models for fields E > 1.0 kV/mm. These data in Figure 4 indicate that the yield stress increases as the electric field increases. The critical shear rates increase with the field in a consistent manner. Thus, in addition to the static and Bingham yield stress, the parameter related to the critical shear rate ($A = \gamma_c^{-1}$) may also be used as an indication of the strength of the ER fluid.

The critical shear rate denotes the shear rate at which the ER structures would begin to form. At high shear rates the hydrodynamic forces prohibit the formation of ER structures. At the critical shear rate the stress minimum is due to the competition between the ER mesostructure destruction, due to hydrodynamics forces, and the ER mesostructure formation, due to the polarization forces. This competition is responsible for the trembling behavior exhibited by the shear stress. Trembling begins at the critical shear rate, which occurs where the hydrodynamic forces are comparable to the polarization forces, which can be quantified by the Mason number. The critical shear rate is a topic for further exploration, but the

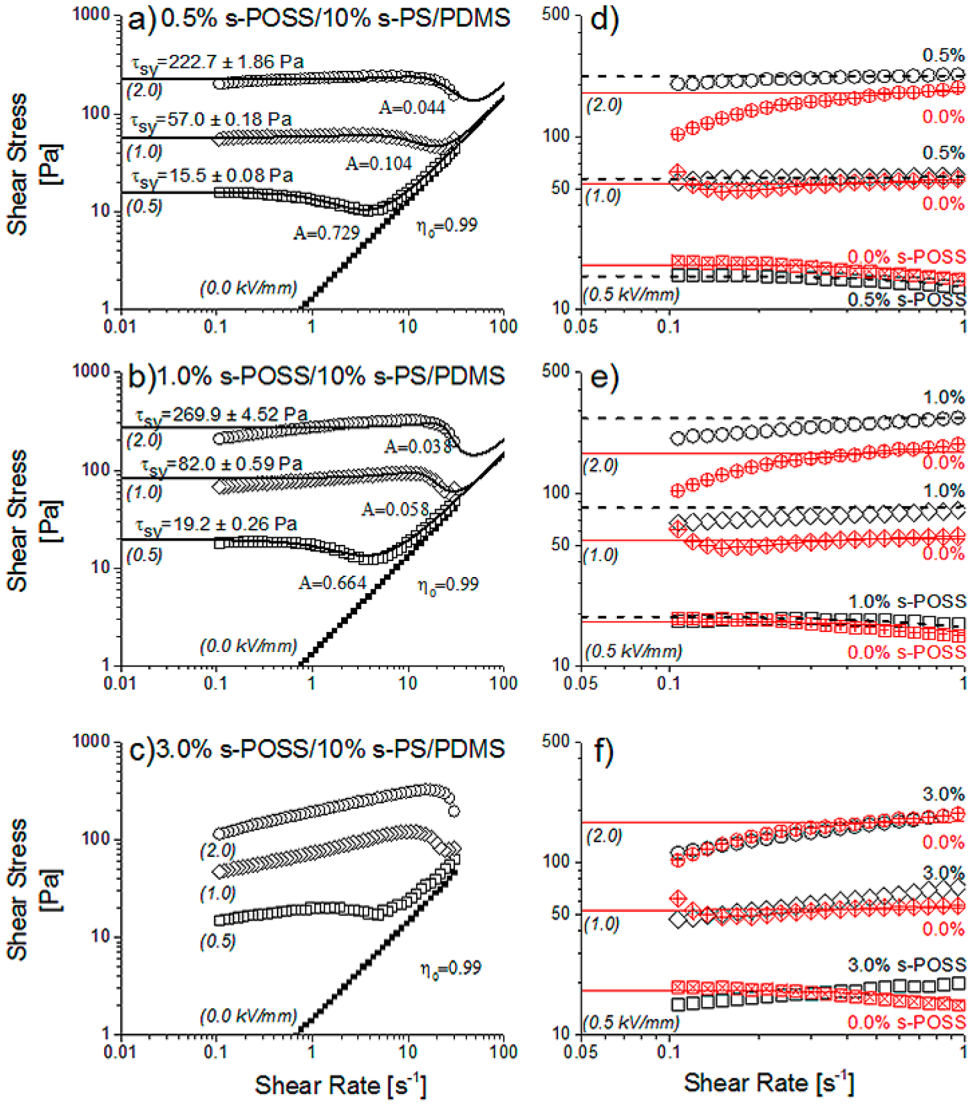

Figure 5. Shear Stress vs Shear Rate flow curves for s-POSS/sPS/PDMS fluids subjected to electric fields *E*: 0, 0.5, 1.0, and 2.0 kV/mm: (a) 0.5% s-POSS; (b) 1.0% s-POSS; (c) 3.0% s-POSS. The solid straight curves are fits to the Seo-Seo model. Confidence Intervals (95%) are included for the static yield stress values based on the fitting. The shear stresses for the ER fluids with and without sPOSS are shown on the right at low shear rates for (d) 0.5% s-POSS, (e) 1.0% s-POSS, and (f) 3.0% s-POSS. The dashed curves and the solid lines are the Seo-Seo Model for the mixtures containing and not containing s-POSS respectively.

qualitative trend noted here is an indication of the enhanced strength of the ER fluid, with the addition of s-POSS.

The increases of the static yield stresses of the ER fluids, under the influence of the electric fields, with increased amounts of s-POSS are shown in Figure 5. Notably, with only 0.5% s-POSS, the static yield stress increases by 46 Pa while subjected to a E = 2.0 kV/mm electric field; for the same applied field the yield stress of the 1% s-POSS suspension increases by 94 Pa. We note that for suspensions containing higher s-POSS concentrations the off-state viscosity (η_0) did not increase, nor should it. Such a significant enhancement of the yield stress of the ER fluid, with virtually no change in the off-state viscosity is noteworthy because this is especially useful for practical ER applications.

It would be expected that higher concentrations of s-POSS, and under increasing electric fields, would lead to increased yield stress. However in s-POSS/s-PS/PDMS ER fluids containing 3% s-POSS, the stress is lower than those exhibited by suspensions containing 1% s-POSS at lower shear rates. This is an interesting observation that we discuss in further detail later. In the meantime we further describe features of this s-POSS/s-PS/PDMS ER suspension. While different analysis or additional measurements of the yield stress are available, we argue that the rheological data in the absence of any model dependent analysis clearly show in Figure 5 d and e that the sPOSS/sPS/PDMS is a superior fluid, specifically for sPOSS concentrations between 0.5 and 2.0%.

The maximum current density that develops in an ER fluid is important because it is associated with failure, due to electric breakdown of the fluid. It may also be used to predict the behavior of the suspensions under the influence of the *E*-field. The field dependence of the maximum current density, plotted in Figure 6, provides additional information about the performance of the ER fluid, the power required for the ER fluid response. The maximum current density remains low, with a slight enhancement at lower fields, in all the suspensions containing s-POSS. We therefore note, from a practical

dx.doi.org/10.1021/am4017544 | ACS Appl. Mater. Interfaces 2013, 5, 8925−8931

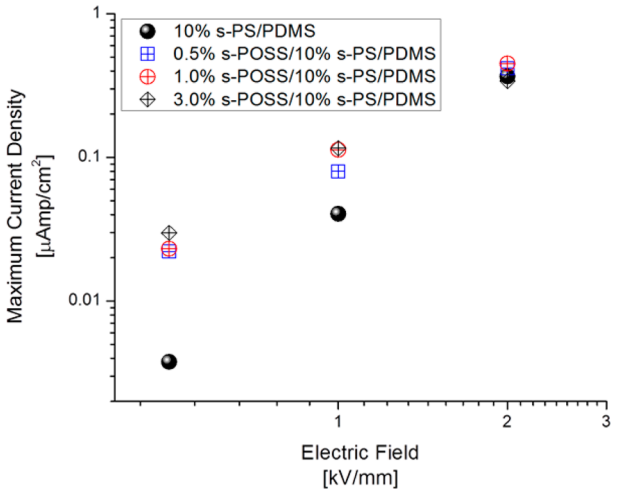

Figure 6. Plot of the electric field dependence of the maximum current density for the ER suspensions.

perspective, that these currents are small, less than 10 mA/cm^2, suggested for the operation of useful devices.[18]

The data in Figure 7 indicate that the static yield stress scales approximately as E^2. This is a slightly stronger field dependence

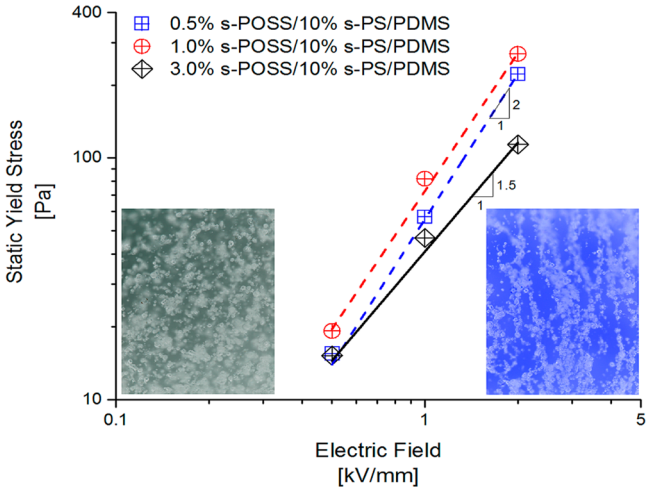

Figure 7. Static yield stresses vs E-field for various suspensions containing different s-POSS concentrations. For 3.0% s-POSS/10% s-PS/PDMS the yield stress is approximated by the stress at the lowest shear rate (γ = 0.1 s^{-1}). The optical micrograph of the fluid is shown on the left in the absence of an E-field (E = 0) and the same fluid is shown on the right in the presence of an E-field (E = 600 V/mm).

than that exhibited by the s-PS/PDMS system. For the highest concentration of s-POSS, the E-field dependence decreases from ~2 (for low fields) to ~1.5 (for high fields). This phenomenon has been observed previously in other ER fluids.[13,19] Clearly one reaches the point of diminishing returns with increasing s-POSS concentration in the suspension.

This observation regarding the ER response with increasing s-POSS, we tentatively propose, would be consistent with the formation of an interfacial layer of s-POSS at the boundaries of the particles. This layer would necessarily not continue to increase in thickness; the excess material would accumulate elsewhere in the suspension. We will address this issue in further detail below. In the meantime we note that the interfacial adsorption is not unexpected based on the findings we reported in our prior study regarding the s-POSS/PS/PDMS system. A fundamental difference here is that the properties of the s-POSS/s-PS/PDMS suspension yield a superior ER fluid.

Dielectric Analysis and Comparison with Models. The enhancement of the ER response of the s-PS/PDMS suspension, through the addition of s-POSS, is clear from the foregoing. However the dielectric properties of the s-POSS/s-PS/PDMS are fundamentally different and provide new insights. The dielectric relaxation spectra, ε'' vs ω, plotted in Figure 8 show the effect of adding s-POSS to the s-PS/PDMS

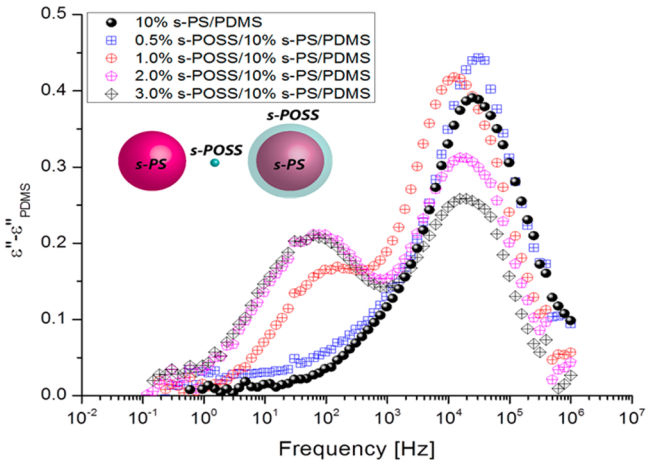

Figure 8. Dielectric loss for s-POSS/s-PS/PDMS, after subtraction of the PDMS contribution.

suspension. Notably a second low frequency peak develops in the spectrum with the addition of s-POSS. The magnitude of this low frequency peak increases with increasing s-POSS. Note, however, that for concentrations >2% s-POSS the low frequency peak remains equal in magnitude to that of the 2 wt % suspension. The behavior of the high frequency peak is different; it decreases in magnitude for concentrations larger than 1 wt %. It is noteworthy that the ER response is comparatively smaller for the higher s-POSS concentration suspensions, where the dielectric response of the substance becomes fundamentally different.

We now examine the origin of the second peak, which is associated with the interfacial adsorption of s-POSS onto the s-PS surfaces. In general the ER effect would be associated with an interfacial polarization process at the interface between the solid and liquid phases.[13] Electrostatic forces at the solid−liquid interface create a mismatch in charge density between the surface and bulk phases, leading to a change in the net polarization of the suspension. The Maxwell−Wagner polarization model predicts that the complex permittivity of a binary suspension would be[13]

$$\varepsilon^* = \varepsilon_H + \left[\frac{\varepsilon_H - \varepsilon_L}{1 + j\omega\tau_0}\right] \quad (3)$$

where τ_0 is the characteristic relaxation time associated with the polarization; ω is the frequency of an applied AC field; ε_L and ε_H are the permittivities of the low field and high field plateau regions, respectively.

While the foregoing describes the case of a binary phase separated suspension, for a ternary mixture, two characteristic relaxations, τ_P and τ_Q, associated with the polarization become

dx.doi.org/10.1021/am4017544 | ACS Appl. Mater. Interfaces 2013, 5, 8925−8931

relevant. Two models have been successfully used to describe cases involving dilute concentrations of dispersed phases or particles in a medium; these are the Stratified model and the Pauly and Schwan (P−S) model.[16,17] With regard to our experimental system, s-POSS/s-PS/PDMS, the Stratified Model assumes that the s-POSS forms a completely separate phase from the s-PS throughout the PDMS host. The P−S model, in contrast, assumes that the s-POSS evenly coats the surfaces of the s-PS particles, with no excess s-POSS remaining in the host phase (s-PS core with an s-POSS shell). The complex permittivity for both models is predicted to be

$$\varepsilon* = \varepsilon_H + \left[\frac{(\varepsilon_L - \varepsilon_I)}{1 + j\omega\tau_P}\right] + \left[\frac{(\varepsilon_I - \varepsilon_H)}{1 + j\omega\tau_Q}\right] + \left[\frac{\kappa_L}{j\omega\varepsilon_V}\right] \quad (4)$$

where κ_L is the low frequency conductivity and κ_m (used in calculation but not shown above) is the conductivity of the matrix or surrounding fluid, which in our case is PDMS. The parameters ε_H, ε_I, ε_L are the high, intermediate, and low frequency permittivities in the plateau regions; ε_V is the vacuum permittivity and is equal to 8.85×10^{-12} F/m. The parameters τ_P and τ_Q are relaxation times.

Using the Pauly−Schwan Model the effect of increasing the amount of s-POSS is illustrated in Figure 9. This model

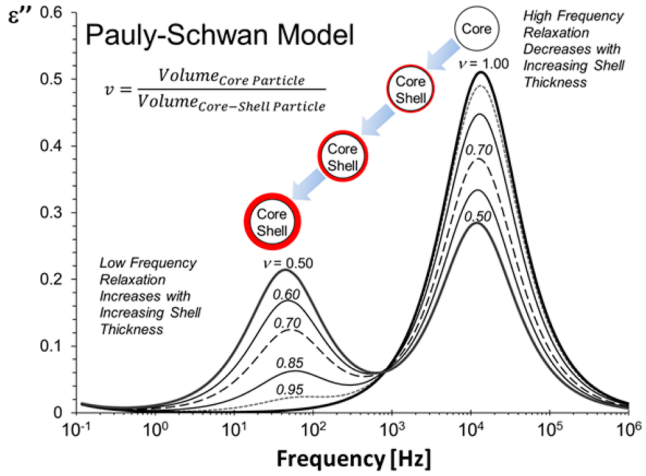

Figure 9. Model Parameters are for Core (Log κ_{core} = −5.58, ε_{core} = 5.15); shell (Log κ_{shell} = −8.5, ε_{shell} = 6); surrounding fluid (Log κ_{fluid} = −14, ε_{fluid} = 3). The volume fraction, Φ, of coated particles and, ν, the ratio of the volumes of the coated particles to the bare particles are varied, for the calculations of ε*.

predicts the existence of a second peak, due to the existence of a shell layer, interfacial adsorption. The calculation was performed for a model system possessing similar relaxation times to that of the s-POSS/s-PS/PDMS ternary mixture. It follows that based on the model system (Figure 9) and the experimentally measured dielectric data (Figure 8), the core (s-PS) possesses a slightly higher conductivity than the shell (s-POSS). As the s-POSS shell increases in thickness, the intensity for the higher frequency peak decreases; concurrently the intensity of the peak for the slower relaxation rates increases.

In light of the foregoing it is evident that the origin of the second peak at lower frequencies is due to the adsorption of s-POSS onto the s-PS surface, thereby forming a core/shell structure. The location of this second peak is determined by the conductivity of the s-POSS shell, relative to that of the s-PS core. Qualitatively, when the layer of s-POSS is completely formed the ER performance ceases to increase; the magnitude of the low frequency peak decreases and that of the high frequency maximum decreases. It is also clear from Figure 8 and Table 1 that the relaxation frequency shifts to lower frequencies as the s-POSS is added; this is due to an increase in the thickness of the coating, reflecting a slower polarization. The significance of this shift of the high frequency peak in the s-POSS/s-PS/PDMS ER fluid is that slower polarizations dominate the ER effect. The peak shift to the left, longer relaxation times, gives an increased relaxation time for the interfacial polarization at the s-PS surface further enhancing the ER effect.

It is important to note that if the s-POSS were assumed not to form an interface with the s-PS, and instead formed a separate phase, then the relaxation time and relaxation frequency, τ_Q, would not change when s-POSS was added. The stratified model predicts no significant changes in τ_Q with increasing s-POSS. For a core−shell particle in an insulating medium the faster relaxation rate is due to the conductivity of either the shell or the core; in the case of s-POSS/s-PS the conductivity of the core is the dominant factor that determines the faster relaxation time (τ_Q) for the ER fluid. This is because the core has a higher conductivity than the shell.

It is clear that the s-POSS/s-PS/PDMS suspensions, with a less conductive s-POSS shell, exhibits stronger ER activity than the s-PS/PDMS suspension. This magnitude of the effect increases with increasing s-POSS, evidently until the surfaces of the s-PS particles are coated. The excess s-POSS at higher concentrations forms a separate phase within the fluid, and the magnitude of the ER effect subsequently decreases. Based on the dielectric spectroscopy measurements, it is evident that the increase in the response is due to an enhancement of the dipolar activity. This weakening at higher concentrations of POSS is due to the decreased conductivity of suspension (excess s-POSS forming a separate phase), which would hinder the stability of the formation of mesostructures, leading to a decrease of the dipolar attractions within the electric field.

Table 1. Dielectric Relaxation Model Parameters for s-POSS ER Fluids

	high frequency relaxation		low frequency relaxation	
s-POSS ER fluid 10% s-PS/PDMS	f_{rel}	intensity	f_{rel}	intensity
0.0% s-POSS	2.47×10^4	0.392 ± 0.020	N/A	N/A
0.5% s-POSS	2.61×10^4	0.438 ± 0.022	N/A	N/A
1.0% s-POSS	1.46×10^4	0.418 ± 0.021	7.9×10^1	0.139 ± 0.007
2.0% s-POSS	1.93×10^4	0.311 ± 0.015	5.9×10^1	0.203 ± 0.010
3.0% s-POSS	1.92×10^4	0.256 ± 0.013	5.7×10^1	0.204 ± 0.010
3.0% s-POSS[a]	1.30×10^3	0.091 ± 0.005	N/A	N/A

[a]s-POSS/PDMS without s-PS.

CONCLUDING REMARKS

Our prior experiments established the fact that the interfacial adsorption of a layer of dipolar molecules onto the surface of PS particles in a PDMS medium changes a previously ER inert suspension (PS/PDMS) to a viable ER fluid: s-POSS/PS/PDMS. We now show that by adding small concentrations (less than 2 wt %) of s-POSS to the ER fluid, s-PS/PDMS, resulted in the formation of a superior ER suspension, s-POSS/s-PS/PDMS, exhibiting a significant improvement in ER activity of over 200% at moderate fields. This behavior is not readily rationalized in terms of current ER theories, which suggests that the properties of the shell, dielectric and conductive, largely determine the yield stress of the system.[7,8] Our results indicate that the conductive properties of the core are very important, otherwise the ER behavior of the s-POSS/PS/PDMS and the s-POSS/s-PS/PDMS suspensions would be comparable. The theories used to rationalize the behavior of the core/shell nanoparticle systems that are responsible for the giant ER (GER) effect are also not applicable to our system. In the GER case, the yield stress scales as E (not E^2), which may not be rationalized in terms of an induced polarization mechanism that seems to be appropriate for our systems. In the end, it is clear that the behavior of the class of ER fluids, formed based on the adsorption of a polar phase, may not be described in terms of the current theories.

ASSOCIATED CONTENT

Supporting Information

Further details are given including particle size distribution, additional dielectric data, and charts. This material is available free of charge via the Internet at http://pubs.acs.org.

AUTHOR INFORMATION

Corresponding Author

*E-mail: pfgreen@umich.edu.

Present Address

[‖]Department of Chemical Engineering, University of Louisiana, Lafayette, Louisiana 70503, United States.

Author Contributions

The manuscript was written through contributions of all authors. All authors have given approval to the final version of the manuscript.

Notes

The authors declare no competing financial interest.

ACKNOWLEDGMENTS

The authors acknowledge support from the University of Michigan and from the Department of Energy, Office of Science, Basic Energy Sciences Program, DOE DE-FG02-07ER46412.

REFERENCES

(1) Larson, R. *The Structure and Rheology of Complex Fluids*; Oxford University Press: New York, 1998; pp 360−376.
(2) Sheng, P.; Wen, W. *Annu. Rev. Fluid Mech.* **2012**, *44*, 143−174.
(3) Kim, Y. D.; Klingenberg, D. J. *J. Colloid Interface Sci.* **1996**, *183*, 568−578.
(4) Espin, M.; Delgado, A.; Plocharski, J. *Rheol. Acta* **2006**, *45*, 865−876.
(5) Cheng, Y.; Liu, X.; Guo, J.; Liu, F.; Li, Z.; Xu, G.; Cui, P. *Nanotechnology* **2009**, *20*, 7.
(6) Huang, X.; Wen, W.; Yang, S.; Sheng, P. *Int. J. Mod. Phys. B* **2007**, *21*, 4907−4913.
(7) Wu, C. W.; Conrad, H. *J. Appl. Phys.* **1997**, *81*, 8057−8063.
(8) Wu, C. W.; Conrad, H. *J. Phys. D: Appl. Phys.* **1998**, *31*, 3312−3315.
(9) Tan, P.; Huang, J.; Liu, D.; Tian, W.; Zhou, L. *Soft Matter* **2010**, *6*, 4800−4806.
(10) McIntyre, C.; Yang, H.; Green, P. F. *ACS Appl. Mater. Interfaces* **2012**, *4*, 2148−2153.
(11) Techaumnat, B.; Takuma, T. *J. Appl. Phys.* **2004**, *96*, 5877−5885.
(12) Akhavan, J. *Proc. Inst. Mech. Eng., Part G* **2007**, *221*, 577−587.
(13) Hao, T. *Electrorheological Fluids*; Elsevier: Amsterdam, The Netherlands, 2005; Vol. *22*, pp 389−398.
(14) Moller, P.; Mewis, J.; Bonn, D. *Soft Matter* **2006**, *2*, 274−283.
(15) Seo, Y. P.; Seo, Y. *Langmuir* **2012**, *28*, 3077−3084.
(16) Tetsuya, H. In *Emulsion Science*; Sherman, P., Ed.; Academic Press: London, U.K., 1968; pp 394−407.
(17) Pauly, H.; Schwan, H. P. *Z. Naturforsch. B* **1959**, *14B*, 125−131.
(18) Weiss, K. D.; Carlson, J. D.; Coulter, J. P. *J. Intell. Mater. Syst. Struct.* **1993**, *4*, 13−34.
(19) Atten, P.; Boissy, C.; Foulc, J. N. *J. Electrost.* **1997**, *40*, 3−12.